Exploring Structural Properties of Cobalt Ferrite Nanoparticles from Natural Sand

IOP Conf. Series: Materials Science and Engineering **515** (2019) 012047 doi:10.1088/1757-899X/515/1/012047

Exploring Structural Properties of Cobalt Ferrite Nanoparticles from Natural Sand

Defi Yuliantika[1], Ahmad Taufiq[1,*], Arif Hidayat[1], Sunaryono[1], Nurul Hidayat[1], Siriwat Soontaranon[2]

[1] Department of Physics, Faculty of Mathematics and Sciences, Universitas Negeri Malang (UM), Jl. Semarang 5, Malang 65145, Indonesia.
[2] Synchrotron Light Research Institute, Muang, Nakhon Ratchasima 30000, Thailand

*Corresponding author's email: ahmad.taufiq.fmipa@um.ac.id

Abstract. In the last years, $CoFe_2O_4$ (cobalt ferrite) nanoparticles become remarkable material due to their performance in various sophisticated applications. In this study, the cobalt ferrite both in powder and ferrofluid phases was successfully synthesized from natural sand. Investigation of the structural properties of the cobalt ferrite was performed using an X-ray diffractometer (XRD) and a small angle X-ray scattering (SAXS) spectrometer to study the crystal structure in the powder and liquid states. The results of the SAXS data analysis using lognormal model revealed that the primary particle size of the cobalt ferrite in powder and ferrofluid had the similar size for the primary particle and fractal dimension, but varied in the secondary particle size. The data analysis using the Rietveld method from XRD data showed that the cobalt ferrite had an inverse spinel cubic structure, respectively. Such data was also confirmed by the data from Fourier transform infrared (FTIR) spectroscopy experiment. Moreover, the data analysis obtained from the ultra-violet visible (UV-Vis) spectroscopy showed that the cobalt ferrite had a semiconductor characteristic with direct band gaps of about 2.27 eV.

Keywords: Cobalt ferrite, powder, ferrofluid, nanoparticle, structure.

1. Introduction

Ferrite nanoparticles are interesting from the view of the application in some disciplines such as biomedical technology [1], nuclear magnetic resonance [2], magnetic fluid [3], hydroelectric energy [4], optoelectronic sensor [5], and catalyst [6]. The synthesis method and material modification and any characterizations of both structure and the other characters of the ferrite nanoparticles should be conducted to support the potential of the recent application. Furthermore, reducing cost during synthesis process of the ferrite nanoparticles becomes one of essentials roles to support the recent application. However, the ferrite nanoparticle synthesis tends to use commercial chemical precursor that is relatively high-cost so far. Therefore, in this research, the precursor was obtained through extraction of natural material in the form of iron sand. This step is important as the solution to utilize the abundant iron sand in Indonesia and further study the development of ferrite nanoparticle synthesis procedure based on iron sand which is more low-cost and efficient than the commercial chemical precursor.

Among the types of ferrites frequently studied by many researchers, cobalt ferrite has excellent characteristic for biomedical technology since it has higher magnetic anisotropy and magnetic moment than the other type of oxide iron [7]. Interestingly, the value of the magnetic anisotropy of cobalt ferrite was 380 kJ/m^3 higher than Fe_3O_4 14 kJ/m^3 [8]. The great anisotropy value causes the magnetic moment of cobalt ferrite takes the relaxation more slowly than the magnetic although with the same magnetic moment size [7]. This excellent magnetic character beneficially implicates especially for the promoter device of cell absorption in the treatment drug delivery [1]. However, unfortunately, some material performances are less optimum since there is a particle aggregation in the liquid and the biodegradable ability is low [7]. Regarding this case, the fabrication of cobalt ferrite in a colloid system called ferrofluid is interesting to be investigated.

Generally, ferrofluid can be said as a soft system for its structure that easily changes in line with the change of physical treatment (temperature and external field). In general, morphology of ferrofluid can be controlled by modifying the particle size [9], while biocompatibility can be reached through ferrofluid fabrication process. Based on the previous research results, ferrofluid showed the excellence in biomedical technology practice such as hyperthermia treatment [10], drug delivery [11], cell separation [12], and magnetic resonance imaging [13]. Therefore, ferrofluid fabrication based on nanocomposite is one of the solutions that should be developed.

In this research, the surface of cobalt ferrite nanoparticles is composited with polyethylene glycol (PEG) and polyvinyl pyrrolidone (PVP) dispersed into water polar medium forming ferrofluids. PEG and PVP were chosen since they have benefits such as a stable hydrophilic polymer in a colloid and they have a biocompatible character so that they are frequently used in the in-vitro and in-vivo application in the pharmaceutical and medical area[14]. Moreover, PEG also functions as a surfactant and deterrent of nanoparticle aggregation in the polar medium [15]. Meanwhile, PVP is built by the long chain structure on monomer N-vinyl pyrrolidone that can be dissolved in the water, and it is non-toxic [14] that is the non-ionic and non-oxide polymer dissolved in the water. Another reason for choosing PVP in this research was because it is easily accessed and low-cost. Furthermore, similar to PEG, this polymer is very biocompatible and a good candidate to modify the surface of magnetic particles to reduce toxicity [16]. Thereby, PVP is very relevant for many applications of pharmacy and biomedical, and amphiphilic that is easily dissolved in both polar and non-polar compounds.

Besides the significant issue related to the use of surfactant, another important issue in the development of ferrofluid research is how to explain the interaction between magnetic particles in the structure and ferrofluid phase [17] becoming the principal basis for a further application. The particle behavior in the ferrofluid is influenced by the interphase between the polymer layer on the surface of magnetic particles with its solvent medium [18]. Hence, in this research, the deep characterization of the structure including optical character is important to be done. Interestingly, characterization of small-angle scattering (SAXS) is also reported in this research to describe the structure and behaviour of cobalt ferrite nanoparticles coated by PEG in a fluid in the form of air and PVP-water polar liquid.

2. Methods

The materials used in this work were iron sand, Hydrochloric acid (HCl, 38%), Ammonium hydroxide (NH_4OH, 25%), Cobalt Chloride ($CoCl_2.6H_2O$), polyethylene glycol (PEG 1000), Polyvinyl pyrrolidone (PVP), distilled water. The cobalt ferrites were synthesized by dissolving 20 grams of natural iron sand into 58 mL of 38% HCl then stirring it in a magnetic stirrer at 300 rpm. Iron chloride solution was filtered by filter paper to separate the insoluble solids of the reactions of product chemical. 15 mL of iron chloride solution was added with 5.06 grams of $CoCl_2.6H_2O$ according to mass stoichiometry. Then through the co-precipitation method, the iron solution was reacted with 5 mL PEG 1000 (conc. 1% in water) at 750 rpm for 2 minutes. PEG was used to coat the surface of nanoparticles to make it soluble in water. The addition of 25 mL of ammonia solution was carried out by continuous sequencing with the stirring process followed by a cobalt ferrite precipitate. The reaction forming cobalt ferrite is given in Equation 1.

$$2\ FeCl_3 + FeCl_2 + 4H_2O + 1.5\ CoCl_2.6H_2O + 11\ NH_4OH \rightarrow 1.5\ CoFe_2O_4 + 11\ NH_4Cl + 9\ H_2O \quad (1)$$

The cobalt ferrite precipitate was neutralized by washing it with the distilled water repeatedly. The samples which achieved normal pH were fabricated in the powder by calcination at 100 °C for 60 minutes and then grinding process to produce fine powder phase. Ferrofluid in this research based on organic polymer PVP as surfactant and water as a dispersant. The fabrication of ferrofluid was by dissolving 0.5 g of PVP in 10 mL of distilled water then stirring 1000 rpm for 10 minutes with thermal treatment to get homogeneity of the solution. Then, the solution was added to 1 g of cobalt ferrite precipitate with continuous stirring for 20 minutes to produce a homogenous ferrofluid phase.

The characterization of the X-ray diffraction (XRD) was performed by PANanalytical X'Pert, and the analysis data was undertaken by Rietica software. The diffraction spectra were recorded at an angle of 2θ, from 20° to 80°, with a Cu-Kα radiation source (wavelength = 1.54056 Å, 40 mA, 40 kV) and step size of 0.02°. Fourier Transform Infrared (FTIR) absorption spectra of the samples were recorded using FTIR spectrometer (Shimaadzu) at the wavenumber range from 4000 to 400 cm^{-1} to study the chemical bonding of cobalt ferrites. Cobalt ferrites were characterized by UV-Visible spectrophotometer for wavelength dependence absorption spectrum. Optical parameters like refractive index, real and imaginary dielectric constants, and optical band gap have been calculated using the Tauc Equation. SAXS experiments were conducted in Synchrotron Light Research Institute, Muang, Nakhon Ratchasima, Thailand. The analysis of the SAXS data was performed using bilognormal and mass fractal models.

3. Results and Discussion

Spectra infrared of cobalt ferrite was characterized by FTIR spectroscopy held in the range of 4000-400 cm^{-1} wavenumber shown by Figure 1. This analysis was used to examine the organic and inorganic bond formed in the cobalt ferrite compound. The organic bond of cobalt ferrite compound is shown by the absorbance peak of 3400-1620 cm^{-1} representing the vibration mode of O-H bond by water molecule absorbed by the surface of nanoparticles during the synthesis process. Besides, the spectrum in the wavenumber of 1498 cm^{-1} is anion carboxylate C-H by PEG polymer coated on the surface of nanoparticles [15]. In this study, PEG functions as a stabilizer to prevent the aggregation of nanoparticles and the active polymer to result in nanoparticles that are water soluble in the ferrofluid system.

The other vibration peaks at 1358 cm^{-1} and 1630 cm^{-1} are COO- symmetric and asymmetric bond group. 1122 cm^{-1} and 2346 cm^{-1} are the vibrations of C-O stretching and CO^2 [19]. Spectrum IR of the metallic bond has two peaks in the range of 400-600 cm^{-1}. The range of 500-385 cm^{-1} is the characteristic of vibration of an atom in the octahedral and tetrahedral positions in the spinel structure [20]. The peak of absorbance at 731 cm^{-1} was Co-O [21] in the octahedral position and at 461 cm^{-1} was Fe-O in the tetrahedral position. These absorbance peaks showed the forming of cobalt ferrite phase having a spinel structure.

Spinel ferrite has face-centered cubic structure and it is noted with MFe_2O_4, where M is metal. Spinel ferrite contains eight tetrahedral positions and 16 octahedral positions. In the spinel ferrite inverse, a half of Fe^{3+} ions were on the tetrahedral position while another half of Fe^{3+} ions and all M^{2+} ions were on the octahedral position. Cobalt ferrite is categorized in the inverse structure of spinel ferrite as shown by IR spectrum from the forming of spinel ferrite compound where Co^{2+} ions were on the octahedral position in the spinel structure [1]. Cobalt ferrite has a spinel structure where atoms will take place on octahedral (B) and tetrahedral (A) positions denoted with $(Fe^{3+})_{\mathbf{A}}(Co^{2+}Fe^{3+})_{\mathbf{B}}O_4$.

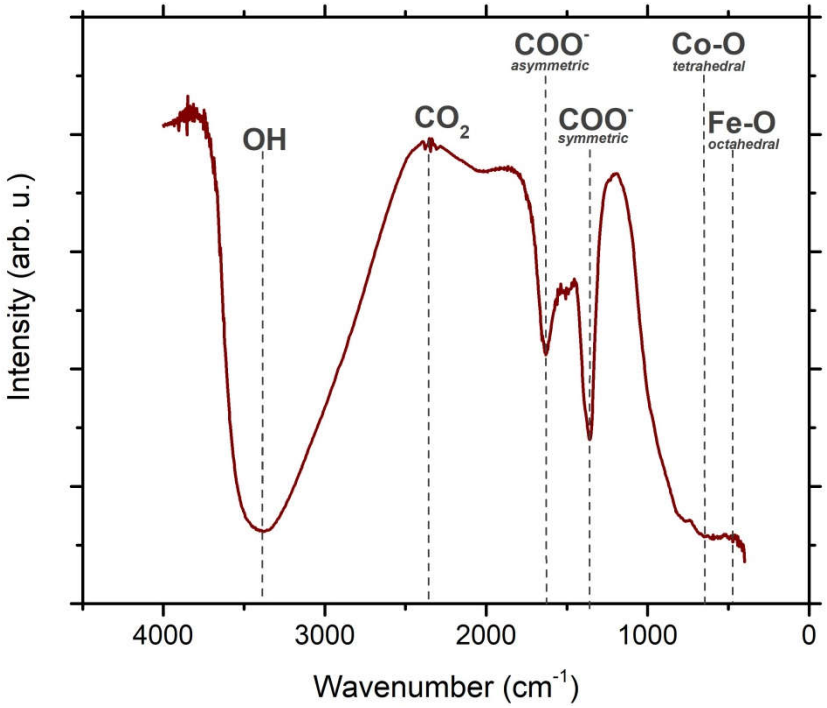

Figure 1. FTIR spectra of the cobalt ferrite particles

Qualitative analysis in examining the structure of cobalt ferrite was done by Rietveld method in XRD data profile shown by figure 3. The diffraction peak pattern corresponded to ICSD 30860 data indicating the forming of spinel structure with the space group of *Fd-3m* (227). The peaks of crystal diffraction appearing were such as (220), (311), (222), (400), (311), (422), (511), (440), (531) and (442) with the not too high peak intensity. This low diffraction intensity is assumed due to the polluter phase by hematite and magnetic [22]. The diffraction peak profile showed the forming of three phases as shown by Figure 2.

In this research, the forming of a compound in the sample resulted in not only cobalt ferrite but also two other phases namely hematite and magnetite with the relatively big enough percentage. The appearance of this polluter phase is because when synthesis process uses iron chloride and cobalt ferrite precursors, the metal ion and oxide that have totally reacted to form cobalt ferrite compound have the excess of iron ions that later react to form [23]. The surface of this magnetite is very reactive so that it easily undergoes oxidation to be hematite when it is subject to air or in the high-temperature place. It is different from the very stable cobalt oxide although it is in the place with oxide. This occurrence was also reported in the research conducted by Estrada *et al*. [8] where the forming of $Co_{0.75}Fe_{2.25}O_4$ compound resulted in two phases namely cobalt ferrite and maghemite. Meanwhile, in this research, the compound with the higher Cobalt content resulted in three phases since the quantity of percentage of iron phase in the precursor based on natural iron sand could not be controlled. The parameter of crystallinity as the data analysis result for each phase formed is presented in Table 1.

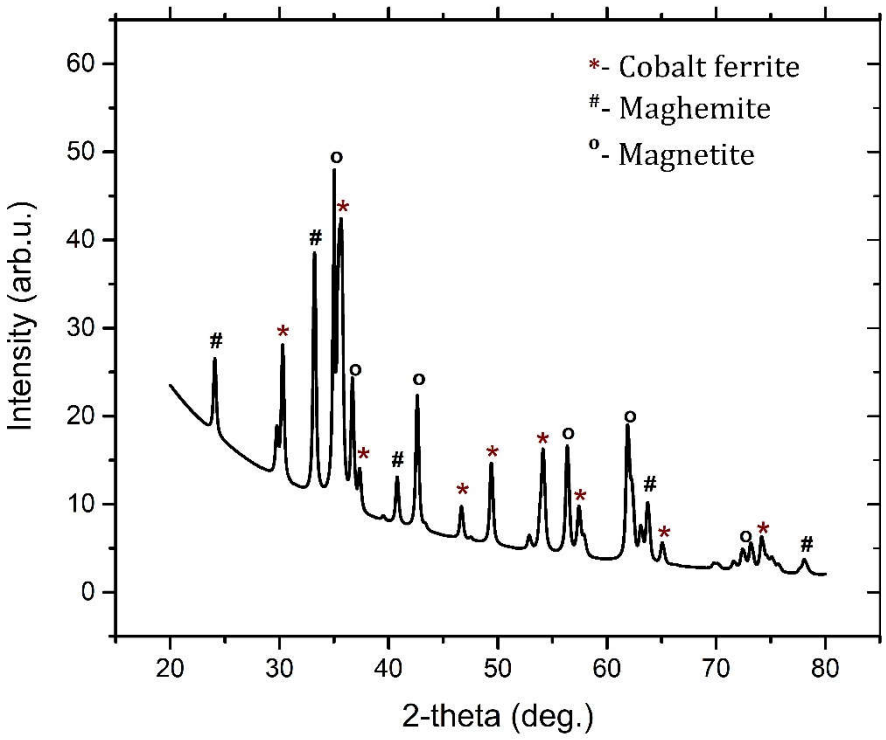

Figure 2. XRD pattern of the cobalt ferrite particles

Table 1. Parameter of cobalt ferrite particles

Phase	Space group	%Wt of Phase	Cell parameter	Particle size (nm)
Cobalt ferrite	*F d-3m*	19.58	$a = b = c = 8.3344$ Å $\alpha = \beta = \gamma = 90^o$	22.87
Magnetite	*F d-3m*	48.64	$a = b = c = 8.4932$ Å $\alpha = \beta = \gamma = 90^o$	27.37
Maghemite	*R -3 c*	31.78	$a = b = 5.0614$, $c = 13.6474$ Å $\alpha = \beta = 90^o$, $\gamma = 120^o$	28.19

Analysis using Rietveld method obtained the size of cobalt ferrite particles was 22.87 nm where the size of cobalt ferrite nanoparticles was smaller than the previous research carried out by Senthil *et al*. [20]. By heating treatment during synthesis, the particle size obtained was 50 nm at temperature of 600 ºC while the synthesis using sol-gel method showed that using simple coprecipitation method has successfully attained the smaller particle size. The analysis result of crystal structure using this diffraction method was strengthened by the analysis result of the structure by X-ray Scattering method using SAXS.

The optical characteristic of cobalt ferrite nanoparticles were investigated using UV-Vis tool. The specimen needed in UV-Vis test was 0.1 gram dissolved in the liquid. The measured UV-Vis absorbance was used to study the effect of cobalt on the optical characteristics such as band gap energy, refractive index, and dielectric content. The curve of the relationship absorbance and wavenumber is shown by Figure 3.

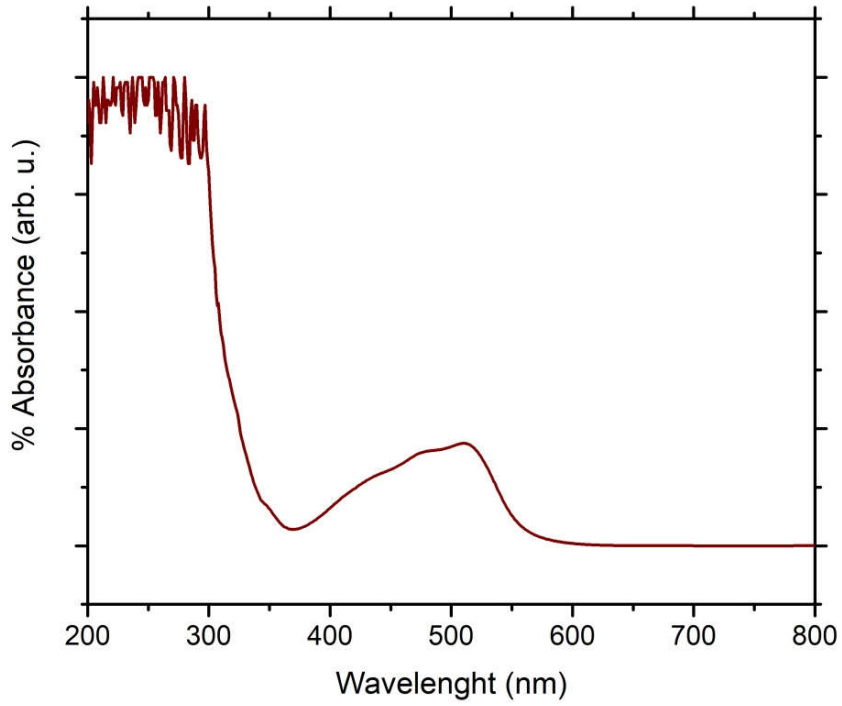

Figure 3. UV-Visible spectrum of cobalt ferrite particles

To gain the information of direct and indirect band, the transition between bands, the analysis of the coefficient value of absorbance α as written in Equation 2 [24].

$$\alpha = \left(\frac{A}{h\upsilon}\right)\left(h\upsilon - E_g\right)^m \tag{2}$$

and the differential form as written in Equation 3.

$$\frac{d\left[\ln(\alpha h\upsilon)\right]}{d(h\upsilon)} = \frac{m}{h\upsilon - E_g} \tag{3}$$

where A is the constant of the comparability of energy, m shows the type of transition (m = 1/2, 3/2, 2 and 3) for the transition of direct allowed, direct forbidden, indirect forbidden or indirect forbidden types [21], $h\upsilon$ is photon energy, E_g is optical band gap. m value was known by plotting the data of the relationship between absorbance differential value and photon energy ($h\upsilon$). The slope of the curve is the value of 1/m and the result was m value was close to 0.5 is shown by Figure 4 indicating cobalt ferrite nanoparticles had the type of transition in the form of the direct band gap. Meanwhile, the optical value of the gap energy was obtained by plotting the curve of the relationship as shown in Figure 5.

Cobalt ferrite nanoparticles have band gap energy of 2.273 eV. Physically, in the direct band gap of hole momentum and electron, there are the same conduction and valence bands; electron needs the energy of 2.273 eV to emit a photon from the valence band to the conduction band. The value of band gap energy of cobalt ferrite was smaller than that of magnetite. The presence of Co ion that changed Fe in the octahedral position enhanced the electron state in the outside orbital area and caused the decrease in band gap energy [8].

The higher value of band gap energy causes certain material needs much more energy to excite an electron from the valence band to conduction band. Therefore, the absorbed light has the higher energy and frequency or shorter wavelength [21]. The absorbance peak in the visible light area opens the potential of cobalt ferrite application in the dye sensitize solar-renewed energy technology [25].

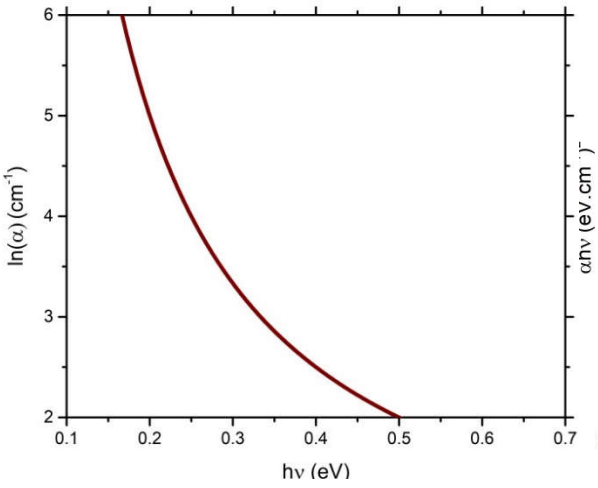

Figure 4. Transition type constant (*m*) of cobalt ferrite particles

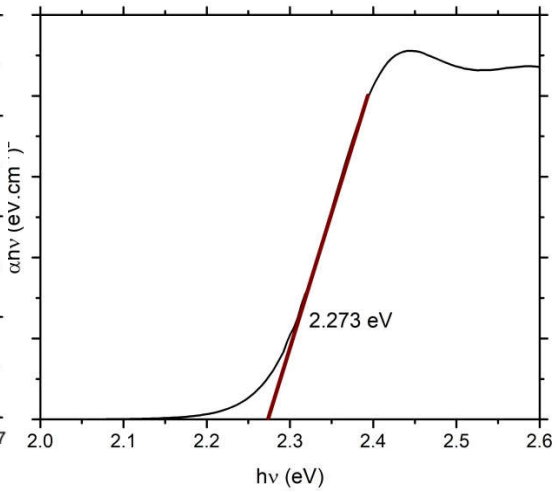

Figure 5. Direct band gap of cobalt ferrite particles

The calculation of refractive index (*n*) value relied on the gap energy value. According to equation of Ravindra, the Equation is (4), where α = 4.048 eV^{-1} and β = -0.62 eV^{-1}. Meanwhile, according to Vandamme, the empirical formulation can be calculated using the Equation (5) with the constant value of variable A = 13.6 eV dan B = 3.4 eV. Meanwhile, according to Ghosh, the empirical relationship is written with the Equation (6) with the parameter value of $A = 25E_g + 212$ and $B = 0.21E_g + 4.25$ [26].

$$n = \alpha + \beta E_g \tag{4}$$

$$n = \sqrt{1 + \left(\frac{A}{E_g + B}\right)^2} \tag{5}$$

$$n^2 - 1 = \frac{A}{\left(E_g + B\right)^2} \tag{6}$$

The value of direct band gap as the result of substitution calculation in the above equation, and the refractive index values as the calculation result using three equations mentioned above are presented in Table 2. The absorbance value obtained from the result of UV-Vis characterization used to know the optical constant value including bias index, absorbance index, dielectric constant until optical conductivity.

Absorbance index by extinction coefficient (*k*) was obtained through Equation 7. The value of absorbance index became the reference for the calculation of material physical parameter namely permittivity as written in Equation 8. Permittivity is a complex variable consisted of the real part (dielectric constant) in Equation 9 and imaginary part (dielectric loss) in the Equation 10. The real and imaginary values of permittivity are related to the constant *n* and *k*.

$$k = \alpha\lambda / 4\pi \quad (7)$$
$$\varepsilon^* = \varepsilon' + i\varepsilon'' \quad (8)$$
$$\varepsilon' = n^2 - k^2 \quad (9)$$
$$\varepsilon'' = 2nk \quad (10)$$

By using the above equation, the optical characteristic of cobalt ferrite nanoparticles is written in Table 3.

Table 2. Refractive index of cobalt ferrite particles.

	Ravindra	Vandamme	Ghosh
A	4.05	13.6	268.82
B	-0.62	3.40	4.7273
refractive index	2.639	2.598	2.547

Table 3. Optical characteristic of cobalt ferrite particles

E_g^{opt}	Refractive index (n)	Extinction coefficient (k)	Dielectric Constant	
			ε' (real)	ε'' (imaginary)
2.273	2.594	1.25×10^{-8}	6.731	6.53×10^{-8}

The other characterization that was also studied in this research was characterization with SAXS technique shown in Figure 6. The *y*-axis is scattering intensity measured as a scattering vector function of the *x*- axis. To represent the distribution of cobalt ferrite nanoparticles in a ferrofluid system and the relationship of interparticle used analysis through the SAXS profile in logarithmic scale. The results of SAXS characterization were analyzed using a distribution model of bilognormal particles referring to the sample characteristic forming the primary and secondary particles combined with mass fractal model [27,28].

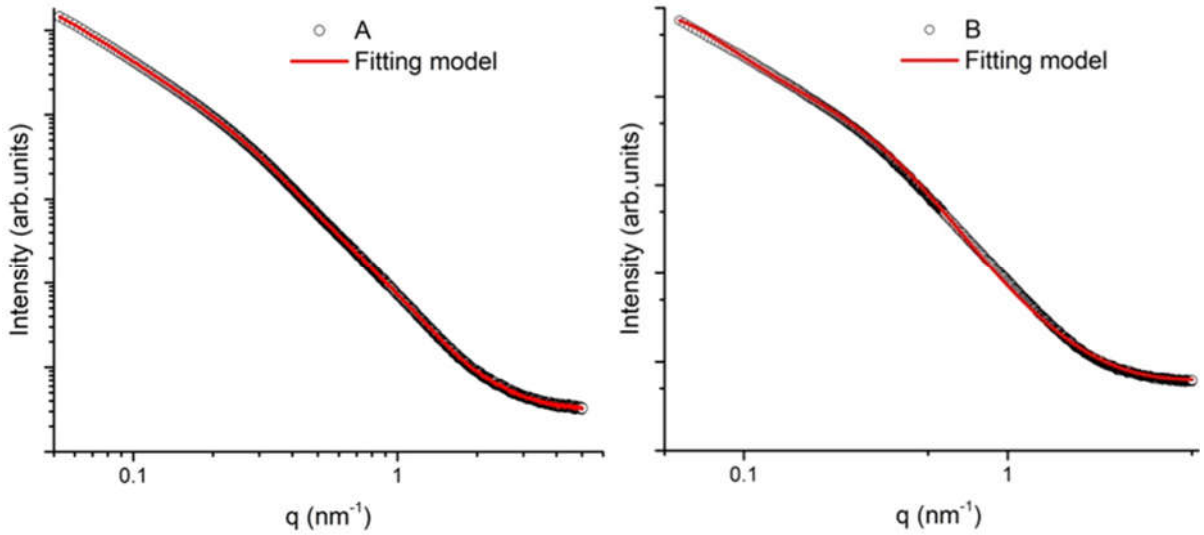

Figure 6. The Result of Fitting lognormal in the sample (A) of cobalt ferrite ferrofluid and (B) cobalt ferrite powder

The analysis results using SAXS provided the information of fractal size and aggregation in the ferrofluid and nanopowder samples. The distribution of particle size modeled in the lognormal distribution with the primary particle size of ferrofluid and powder had a similar size which was 2.3 nm while the secondary particle size was different. The distribution of particle size in the sample can be seen through polidispersity parameter where the primary particle size of the character is more monodispersed than secondary particles. The particle structure in both samples was modeled in the form of mass fractal. The analysis results showed that parameter *D* of both samples were almost similar that was ~3. Interestingly, both samples had different secondary particle size. This case was indicated by the secondary particle size which was 29.8 nm for ferrofluid sample and 83.8 nm for nanopowder sample. The smaller secondary particle size in the ferrofluid was achieved because the surfactant process successfully prevented the aggregation of magnetic particles to form bigger particle grain [28]. In this research, the space between building block of powder sample had the bigger value than that of ferrofluid. Theoretically, this case happened ferrofluid had the smaller aggregation value than powder sample due to PVP and PEG surfactant that were absent in the powder sample.

The result of data analysis by scattering method using SAXS provided broader information related to the characteristic of particle structure than X-ray diffraction method. The particle size of XRD result was in the range of ~27 nm where it is related to the secondary particle size of the sample. Meanwhile, the dimension of fractal *D* around the value of 3 showed that the particles formed the building block structure with the growth of particles in the field orientation of 3-dimension. Meanwhile, the *D* value around 2 formed disc-like macrostructure [29].

4. Conclusion

The characteristics of particle structure examined by diffraction method through X-ray diffraction and scattering methods using SAXS showed the broad structural parameter. The result of XRD analysis informed the forming of crystal phase consisted of cobalt ferrites, magnetite and maghemite phases with the particle mean size of ~20 nm. Meanwhile, the analysis using SAXS resulted in the primary and secondary sizes of both powder and fluid samples that had the distribution of primary particle size that was more homogeny than that of secondary particle size. In 3-dimension model, particles formed fractal dimension with the size of ~3 nm and ~12 nm in the cluster aggregation form with the size where the space between clusters was separated at the range of 100-200 nm. The optical characteristics using UV-Vis showed that the sample had the transition with the type of direct band gap with the value of band gap energy of ~2.27 eV in the range of appearing light absorbance. Besides, the values of bias index, absorbance index, and dielectric constant of cobalt ferrite nanoparticles were successfully reported in this research.

References

[1] Srinivasan S Y, Paknikar K M, Bodas D and Gajbhiye V 2018 Applications of cobalt ferrite nanoparticles in biomedical nanotechnology *Nanomed.* **13** 1221–38

[2] Korneisel R, Nlebedim C, Prabhu Gaunkar N and Jiles D 2018 Analysis of the magnetic and ringing properties of nickel-zinc-ferrite for use in pulsed nuclear magnetic resonance applications *Bull. Am. Phys. Soc.*

[3] Kharat P B, Somvanshi S B, Kounsalye J S, Deshmukh S S, Khirade P P and Jadhav K M 2018 Temperature dependent viscosity of cobalt ferrite / ethylene glycol ferrofluids p 050044

[4] Kotnala R K and Shah J 2016 Green hydroelectrical energy source based on water dissociation by nanoporous ferrite: Green hydroelectrical energy source *Int. J. Energy Res.* **40** 1652–61

[5] Manikandan V, Sikarwar S, Yadav B C and Mane R S 2018 Fabrication of tin substituted nickel ferrite (Sn-$NiFe_2O_4$) thin film and its application as opto-electronic humidity sensor *Sens. Actuators Phys.* **272** 267–73

[6] Yue Q, Liu C, Wan Y, Wu X, Zhang X and Du P 2018 Defect engineering of mesoporous nickel ferrite and its application for highly enhanced water oxidation catalysis *J. Catal.* **358** 1–7

[7] Baldi G, Bonacchi D, Franchini M C, Gentili D, Lorenzi G, Ricci A and Ravagli C 2007 Synthesis and Coating of Cobalt Ferrite Nanoparticles: A First Step toward the Obtainment of New Magnetic Nanocarriers *Langmuir* **23** 4026–8
[8] Estrada S O, Huerta-Aguilar C A, Pandiyan T, Corea M, Reyes-Domínguez I A and Tavizon G 2017 Tuning of the magnetic response in cobalt ferrite $Co_xFe_{3-x}O_4$ by varying the Fe^{2+} to Co^{2+} molar ratios: Rietveld refinement and DFT structural analysis *J. Alloys Compd.* **695** 2706–16
[9] Safran S A 2003 Ferrofluids: Magnetic strings and networks *Nat. Mater.* **2** 71
[10] Kandasamy G, Sudame A, Bhati P, Chakrabarty A, Kale S N and Maity D 2018 Systematic magnetic fluid hyperthermia studies of carboxyl functionalized hydrophilic superparamagnetic iron oxide nanoparticles based ferrofluids *J. Colloid Interface Sci.* **514** 534–43
[11] Komaee A 2017 Feedback Control for Transportation of Magnetic Fluids With Minimal Dispersion: A First Step Toward Targeted Magnetic Drug Delivery *IEEE Trans. Control Syst. Technol.* **25** 129–44
[12] Zhao W, Cheng R, Lim S H, Miller J R, Zhang W, Tang W, Xie J and Mao L 2017 Biocompatible and label-free separation of cancer cells from cell culture lines from white blood cells in ferrofluids *Lab. Chip* **17** 2243–55
[13] Hayashi K, Sakamoto W and Yogo T 2016 Smart Ferrofluid with Quick Gel Transformation in Tumors for MRI-Guided Local Magnetic Thermochemotherapy *Adv. Funct. Mater.* **26** 1708–18
[14] Obaidat R M, AlTaani B and Ailabouni A 2017 Effect of different polymeric dispersions on In-vitro dissolution rate and stability of celecoxib class II drug *J. Polym. Res.* **24**
[15] Spizzo F, Sgarbossa P, Sieni E, Semenzato A, Dughiero F, Forzan M, Bertani R and Del Bianco L 2017 Synthesis of Ferrofluids Made of Iron Oxide Nanoflowers: Interplay between Carrier Fluid and Magnetic Properties *Nanomaterials* **7** 373
[16] İşçi S, İşçi Y and Bekaroğlu M G 2017 Particle interactions of polyvinylpyrrolidone-coated iron oxide particles as magnetic drug delivery agents *Appl. Phys. A* **123** 534
[17] Butter K, Bomans P H H, Frederik P M, Vroege G J and Philipse A P 2003 Direct observation of dipolar chains in iron ferrofluids by cryogenic electron microscopy *Nat. Mater.* **2** 88
[18] Filomeno C L, Kouyaté M, Peyre V, Demouchy G, Campos A F C, Perzynski R, Tourinho F A and Dubois E 2017 Tuning the Solid/Liquid Interface in Ionic Colloidal Dispersions: Influence on Their Structure and Thermodiffusive Properties *J. Phys. Chem. C* **121** 5539–50
[19] Rouhani A R, Esmaeil-Khanian A H, Davar F and Hasani S 2018 The effect of agarose content on the morphology, phase evolution, and magnetic properties of $CoFe_2O_4$ nanoparticles prepared by sol-gel autocombustion method *Int. J. Appl. Ceram. Technol.* **15** 758–65
[20] Senthil V P, Gajendiran J, Raj S G, Shanmugavel T, Ramesh Kumar G and Parthasaradhi Reddy C 2018 Study of structural and magnetic properties of cobalt ferrite ($CoFe_2O_4$) nanostructures *Chem. Phys. Lett.* **695** 19–23
[21] Anjum S, Tufail R, Rashid K, Zia R and Riaz S 2017 Effect of cobalt doping on crystallinity, stability, magnetic and optical properties of magnetic iron oxide nano-particles *J. Magn. Magn. Mater.* **432** 198–207
[22] Covaliu C I, Jitaru I, Paraschiv G, Vasile E, Biriş S-Ş, Diamandescu L, Ionita V and Iovu H 2013 Core–shell hybrid nanomaterials based on $CoFe_2O_4$ particles coated with PVP or PEG biopolymers for applications in biomedicine *Powder Technol.* **237** 415–26
[23] Nlebedim I C, Snyder J E, Moses A J and Jiles D C 2012 Effect of deviation from stoichiometric composition on structural and magnetic properties of cobalt ferrite, $Co_xFe_{3-x}O_4$ ($x = 0.2$ to 1.0) *J. Appl. Phys.* **111** 07D704
[24] Singh R, Verma R, Kaushik A, Sumana G, Sood S, Gupta R K and Malhotra B D 2011 Chitosan–iron oxide nano-composite platform for mismatch-discriminating DNA hybridization for Neisseria gonorrhoeae detection causing sexually transmitted disease *Biosens. Bioelectron.* **26** 2967–74

[25] Habibi M H and Parhizkar H J 2014 FTIR and UV–vis diffuse reflectance spectroscopy studies of the wet chemical (WC) route synthesized nano-structure $CoFe_2O_4$ from $CoCl_2$ and $FeCl_3$ *Spectrochim. Acta. A. Mol. Biomol. Spectrosc.* **127** 102–6
[26] Foo K L, Hashim U, Muhammad K and Voon C H 2014 Sol–gel synthesized zinc oxide nanorods and their structural and optical investigation for optoelectronic application *Nanoscale Res. Lett.* **9** 429
[27] Taufiq A, Sunaryono, Hidayat N, Hidayat A, Putra E G R, Okazawa A, Watanabe I, Kojima N, Pratapa S and Darminto 2017 Studies on Nanostructure and Magnetic Behaviors of Mn-Doped Black Iron Oxide Magnetic Fluids Synthesized from Iron Sand *Nano* **12** 1750110
[28] Sunaryono, Taufiq A, Mufti N, Susanto H, Putra E G R, Soontaranon S and Darminto 2018 Contributions of TMAH Surfactant on Hierarchical Structures of PVA/Fe_3O_4–TMAH Ferrogels by Using SAXS Instrument *J. Inorg. Organomet. Polym. Mater.*
[29] Putra E G R, Seong B S, Shin E, Ikram A, Ani S A and Darminto 2010 Fractal Structures on Fe_3O_4 Ferrofluid: A Small-Angle Neutron Scattering Study *J. Phys. Conf. Ser.* **247** 012028

Acknowledgments
This work was supported by a research grant for AT "PSNI" from KEMENRISTEKDIKTI RI in 2018.